

Precision calculation of $np \rightarrow d\gamma$ cross section for Big-Bang Nucleosynthesis

Gautam Rupak
*Department of Physics,
University of Washington,
Seattle, WA 98195*

Abstract

An effective field theory calculation of the $np \rightarrow d\gamma$ cross section accurate to 1% for center of mass energy $E \lesssim 1$ MeV is presented. At these energies, which are relevant for big-bang nucleosynthesis, isovector magnetic transitions $M1_V$ and isovector electric transitions $E1_V$ give the dominant contributions. The $M1_V$ amplitude is calculated up to next-to-next-to-leading order (N²LO) and the associated four-nucleon-one-photon counterterm is determined from the cold neutron capture rate. The $E1_V$ amplitude is calculated up to N⁴LO. The four-nucleon-one-photon counterterm contribution to $E1_V$ is determined from the related deuteron photodisintegration reaction $\gamma d \rightarrow np$.

September 1999

I. INTRODUCTION

Big-bang nucleosynthesis (BBN) is a cornerstone of big-bang cosmology [1]. Primordial deuterium production is very sensitive to the baryon density of the universe and thus the BBN prediction of deuterium abundance can be used to infer this baryon density. These deuterium abundance calculations use the cross section for $np \rightarrow d\gamma$ as an input. Thus, an accurate estimation of the $np \rightarrow d\gamma$ cross section is essential to the BBN prediction of abundance of light elements. At the energies relevant for BBN, $0.02 \lesssim E \lesssim 0.2$ MeV, this reaction is not well-measured experimentally and there are significant theoretical uncertainties [1]. For example, in the model calculation of Smith, Kawano and Malaney [2] an error of 5% was assigned to the cross section for $np \rightarrow d\gamma$. A recent model independent calculation by Chen and Savage [3], using a low energy effective field theory (EFT) predicted a theoretical uncertainty of 4%. This work is a one higher order calculation in the perturbative expansion of the EFT used in Ref. [3]. The theoretical uncertainty is estimated to be $\lesssim 1\%$ for center of mass energies $E \lesssim 1$ MeV.

For thermal neutrons ($E \sim 10^{-8}$ MeV), the cross section for $np \rightarrow d\gamma$ is dominated by the isovector magnetic transition $M1_V$ from the 1S_0 isovector channel to the 3S_1 isoscalar channel. At higher energies, $E \sim 1$ MeV, the cross section for $np \rightarrow d\gamma$ is dominated by isovector electric transitions $E1_V$ from the isovector P -wave to 3S_1 channel. At the energies relevant for BBN, the $M1_V$ and $E1_V$ transitions give comparable contributions.

Effective field theory is a useful tool in the study of physical processes with a clear separation of scales. This is the case for the reaction $np \rightarrow d\gamma$. At energies relevant for BBN, the nucleon center of mass momentum $p \sim 30$ MeV, the deuteron binding momentum $\gamma_t \sim 45$ MeV and the inverse of the singlet channel 1S_0 neutron-proton scattering length $1/a^{exp} \sim 8$ MeV are all much smaller than the mass of the lightest meson, the pion with mass $m_\pi \sim 140$ MeV. Thus a low energy EFT can be constructed by integrating out the pions and other heavier degrees of freedom out of the theory. The strong interaction of the nucleons is then described by four-nucleon operators [4,5]. The effects of the particles that were integrated out of the theory are encoded in a perturbative expansion of local operators, where the expansion parameter is expected to be Q/m_π with $p, \gamma_t, 1/(a^{exp}) \sim Q$. The perturbative description of the low energy physics then allows a systematic estimation of errors at any order in the perturbation.

Recently there has been much discussion [3–6] about the role EFT can play in improving the 'traditional' results obtained using effective-range theory (ERT) for low energy observables in the two nucleon system. It was shown in Ref. [7] that for nucleon-nucleon scattering, ERT and low energy EFT are equivalent. In some processes involving external currents, e.g. electron-deuteron scattering, the ERT amplitude differs from EFT results due to the absence of two-body current operators. The most general set of allowed multi-nucleon-external-field operators contains operators that need not be related to the nucleon-nucleon scattering operators, included in ERT, by gauging the derivatives through minimal photon coupling. Including multi-nucleon-external-field operators, e.g. two-body currents, is straightforward in EFT. The deviation of the ERT result from EFT due to the absence of two-body current operators, which are not related to nucleon-nucleon scattering operators by gauge transformation, will be greater if these operators appear at lower order in the perturbative EFT expansion. For example, in the EFT without dynamical pions a four-nucleon-one-photon

operator contributes to deuteron quadrupole moment μ_Q at next-to-leading order (NLO) [5]. The absence of such a operator in the ERT could be responsible for potential models' under prediction of μ_Q by about 5% [5,8] in the impulse approximation [9,10]. In $np \rightarrow d\gamma$, the $M1_V$ transition amplitude also involves a four-nucleon-one-photon operator at NLO in the EFT that is not included in the ERT. This operator contributes about 5% to the cold neutron capture cross section $\sigma^{exp} = 334.2$ mb and an about 2% at energy $E \sim 0.5$ MeV. On the other hand, the $E1_V$ amplitude can be written entirely in terms of nucleon-nucleon scattering operators up to N³LO and reduces to the ERT result at this order.

The $M1_V$ transition amplitude has been calculated up to NLO [3,11,12]. The unknown coupling L_1^{M1} , associated with a four-nucleon-one-photon operator, appearing at this order can be determined from the cold neutron capture rate of $\sigma^{exp} = 334.2 \pm 0.5$ mb [13] at incident neutron speed $v = 2200$ m/s. The $E1_V$ transition amplitude has been calculated up to N³LO [3]. In this work, we calculate the $M1_V$ transition amplitude up to N²LO and the $E1_V$ transition amplitude up to N⁴LO. For the $M1_V$ amplitude, there is a new unknown coupling $L_3^{M1_V}$ at N²LO. Only a linear combination of $L_1^{M1_V}$ and $L_3^{M1_V}$ contributes at very low momentum. We derive perturbative constrains [12,14] on these couplings to reproduce the low energy cross section σ^{exp} . For the $E1_V$ transition, there is a coupling $L_1^{E1_V}$ at N⁴LO that is not determined from nucleon-nucleon scattering data. We determine L_1^{E1} from a χ^2 fit to data [15] for the related process of deuteron photodisintegration $\gamma d \rightarrow np$.

The organization of the paper is as follows: We first describe the relevant Lagrangian and the power counting rules in Section II. This section is rather technical and primarily used to define various parameters that enter the expression for the cross section. The calculation of the total cross section is presented in Subsections III A, III B and III C. The renormalization group (RG) flow of the couplings is discussed in some detail, and from the RG analysis constraints on some of the couplings are derived. In Subsection III D, all the remaining couplings are determined. We tabulate the calculated cross section for some energies relevant for BBN, discuss the theoretical errors, and compare our results with the corresponding values from the on-line database at NNDC [16] in Section IV. Summary and conclusions follow in Section V.

II. THE LAGRANGIAN AND POWER COUNTING

For an EFT calculation we need a Lagrangian, and a set of power counting rules that determine the relative sizes of diagrams contributing to a physical process. In addition to the nucleon kinetic term

$$\mathcal{L}_1 = N^\dagger \left[iD_0 + \frac{\mathbf{D}^2}{2M_N} - \frac{D_0^2}{2M_N} \right] N, \quad (2.1)$$

where the covariant derivative is

$$D^\mu = \partial^\mu + ie \frac{1 + \tau_3}{2} A^\mu, \quad (2.2)$$

the Lagrangian relevant for radiative capture process $np \rightarrow d\gamma$ and the photodisintegration of the deuteron $\gamma d \rightarrow np$ can be divided into (a) a Lagrangian \mathcal{L}_2^S contributing to nucleon-nucleon scattering in the 3S_1 and 1S_0 channels, (b) a Lagrangian \mathcal{L}_2^P contributing to nucleon-nucleon scattering in relative angular momentum states 3P_0 , 3P_1 , 3P_2 and (c) a Lagrangian

\mathcal{L}_2^{EM} describing two-body currents that are not contained in the two previous Lagrangians. Note that the D_0^2 term in Eq. (2.1) includes all the relativistic corrections to the nucleon kinetic energy [5].

A. Lagrangian: \mathcal{L}_2^S

We start by describing the Lagrangian contributing to the final or initial state nucleon-nucleon interaction responsible for binding the deuteron. In the 3S_1 channel, up to N⁴LO:

$$\begin{aligned}
\mathcal{L}_2^{({}^3S_1)} = & -C_0(N^T P_i N)^\dagger (N^T P_i N) + \frac{C_2}{2} \left[(N^T \mathcal{O}_i^{(2)} N)^\dagger (N^T P_i N) + h.c. \right] \\
& -C_4(N^T \mathcal{O}_i^{(2)} N)^\dagger (N^T \mathcal{O}_i^{(2)} N) - \frac{\tilde{C}_4}{2} \left[(N^T \mathcal{O}_i^{(4)} N)^\dagger (N^T P_i N) + h.c. \right] \\
& + \frac{C_6}{2} \left[(N^T \mathcal{O}_i^{(4)} N)^\dagger (N^T \mathcal{O}_i^{(2)} N) + h.c. \right] + \frac{\tilde{C}_6}{2} \left[(N^T \mathcal{O}_i^{(6)} N)^\dagger (N^T P_i N) + h.c. \right] \quad (2.3) \\
& -C_8^\alpha (N^T \mathcal{O}_i^{(4)} N)^\dagger (N^T \mathcal{O}_i^{(4)} N) - \frac{C_8^\beta}{2} \left[(N^T \mathcal{O}_i^{(6)} N)^\dagger (N^T \mathcal{O}_i^{(2)} N) + h.c. \right] \\
& + C_2^{(sd)} \left[(N^T P_i N)^\dagger (N^T \mathcal{O}^{xyj} N) \mathcal{T}^{ijxy} + h.c. \right] ,
\end{aligned}$$

where summation over the repeated indices is implied. The P_i matrices are used to project onto the 3S_1 state,

$$P_i \equiv \frac{1}{\sqrt{8}} \sigma_2 \sigma_i \otimes \tau_2 , \quad \text{Tr}[P_i^\dagger P_j] = \frac{1}{2} \delta_{ij} , \quad (2.4)$$

where the σ matrices act on the nucleon spin space and the τ matrices act on the nucleon isospin space. The Galilean invariant covariant derivative operators are defined as:

$$\begin{aligned}
\mathcal{O}_i^{(2)} &= \frac{1}{4} \left[\overleftarrow{\mathbf{D}}^2 P_i - 2 \overleftarrow{\mathbf{D}} P_i \overrightarrow{\mathbf{D}} + P_i \overrightarrow{\mathbf{D}}^2 \right] \\
\mathcal{O}_i^{(4)} &= \frac{1}{16} \left[\overleftarrow{\mathbf{D}}^4 P_i - 4 \overleftarrow{\mathbf{D}}^3 P_i \overrightarrow{\mathbf{D}} + 6 \overleftarrow{\mathbf{D}}^2 P_i \overrightarrow{\mathbf{D}}^2 - 4 \overleftarrow{\mathbf{D}} P_i \overrightarrow{\mathbf{D}}^3 + P_i \overrightarrow{\mathbf{D}}^4 \right] \quad (2.5) \\
\mathcal{O}_i^{(6)} &= \frac{1}{64} \left[\overleftarrow{\mathbf{D}}^6 P_i - 6 \overleftarrow{\mathbf{D}}^5 P_i \overrightarrow{\mathbf{D}} + 15 \overleftarrow{\mathbf{D}}^4 P_i \overrightarrow{\mathbf{D}}^2 - 20 \overleftarrow{\mathbf{D}}^3 P_i \overrightarrow{\mathbf{D}}^3 \right. \\
&\quad \left. + 15 \overleftarrow{\mathbf{D}}^2 P_i \overrightarrow{\mathbf{D}}^4 - 6 \overleftarrow{\mathbf{D}} P_i \overrightarrow{\mathbf{D}}^5 + P_i \overrightarrow{\mathbf{D}}^6 \right] \\
\mathcal{O}^{xyj} &= \frac{1}{4} \left[\overleftarrow{\mathbf{D}}^x \overleftarrow{\mathbf{D}}^y P_j - \overleftarrow{\mathbf{D}}^x P_j \overrightarrow{\mathbf{D}}^y - \overleftarrow{\mathbf{D}}^y P_j \overrightarrow{\mathbf{D}}^x + P_j \overrightarrow{\mathbf{D}}^x \overrightarrow{\mathbf{D}}^y \right] \\
\mathcal{T}^{ijxy} &= \left(\delta^{ix} \delta^{jy} - \frac{1}{n-1} \delta^{ij} \delta^{xy} \right) ,
\end{aligned}$$

where n is the number of space-time dimensions. For the $M1_V$ transition there is also initial or final state nucleon-nucleon interaction in the 1S_0 channel and the Lagrangian has the same form as the one described in Eq. (2.3), with the corresponding projections onto the 1S_0 channel. Note that there is no corresponding S - D mixing term, $C_2^{(sd)}$, in the 1S_0 channel.

The power counting is as follows: The expansion parameter is Q/Λ . The nucleon center of mass momentum p , the deuteron binding momentum γ_t , the inverse of the 1S_0 channel

scattering length $1/a^{exp}$ and the renormalization scale μ are formally considered $\mathcal{O}(Q)$ and $\Lambda \sim m_\pi/2$ for this low energy EFT (the factor of half comes from the analytic structure of the one pion graph contributions). The couplings C_{2n} scale as $1/Q^{n+1}$, \tilde{C}_{2n} scale as $1/Q^n$ and $C_2^{(sd)}$ scales as $1/Q$. For the low energy theory, we formally take $m_\pi/M_N \sim Q/\Lambda$. Thus, relativistic corrections which come in as $p^2/M_N^2 = p^2/m_\pi^2 \times m_\pi^2/M_N^2$ and γ_t^2/M_N^2 contribute at N⁴LO.

It is a feature of the KSW power counting that the EFT couplings associated with S -state interactions scale with some powers of Q . This is because the couplings are fine-tuned to reproduce the large scattering lengths that one sees in the 1S_0 and 3S_1 channels. In order to reproduce the exact deuteron pole, the coefficients C_{2n} are expanded in powers of Q :

$$\begin{aligned} C_0 &= C_{0,-1} + C_{0,0} + \dots \\ C_2 &= C_{2,-2} + C_{2,-1} + \dots \\ &\vdots \end{aligned} \tag{2.6}$$

where the second subscript denotes the Q scaling. The EFT couplings C_{2n} are determined by matching [4,5,14] the nucleon-nucleon scattering amplitude calculated in EFT and that obtained from the ERE [17]:

$$p \cot \delta = -\gamma_t + \frac{1}{2}\rho_d (p^2 + \gamma_t^2) + \frac{1}{2}w_2 (p^2 + \gamma_t^2)^2 + \dots \tag{2.7}$$

To the order we are working, the deuteron binding momentum $\gamma_t \approx \gamma - \gamma^3/(8M_N^2)$, where $\gamma = \sqrt{M_N B}$ and $B = 2.2246$ MeV [18] is the deuteron binding energy. The coupling $C_2^{(sd)} = 3\eta_d/(\sqrt{2}\gamma^2)$ is determined from the S - D mixing parameter $\bar{\epsilon}_1$ [5,12,19], where $\eta_d = 0.02534$ is the D -wave to S -wave ratio at the deuteron pole [18]. Notice that $C_2^{(sd)}$ is smaller than naive power counting estimate because of the smallness of the parameter η_d .

For our calculation, we need the 3S_1 channel initial or final state interaction up to N⁴LO and the 1S_0 interaction up to N²LO. In the 3S_1 channel, at N⁴LO only four experimental inputs (γ , ρ_d , w_2 and η_d) enter the scattering amplitude. The EFT couplings that depend on the high energy scale can all be expressed in terms of these four parameters. However, only the combinations $C_4 + \tilde{C}_4$ and $C_8^\alpha + C_8^\beta \equiv C_8$ contribute to nucleon-nucleon scattering and so nucleon-nucleon scattering data can not be used to separate C_4 from \tilde{C}_4 , and C_8^α from C_8^β . We use the effective range $\rho_d = 1.764$ fm and shape parameter $w_2 = 0.778$ fm³ [18]. In the 1S_0 channel, at N²LO the nucleon-nucleon scattering amplitude is completely determined by the scattering length a^{exp} and the effective range r_0 . The EFT couplings C_{2n} are determined in terms of these two parameters. Note that the experimentally measured scattering length a^{exp} , for neutron-proton scattering in the singlet channel 1S_0 , gets about a 3% contribution from magnetic moment interaction [10]. Isospin-breaking single magnetic photon exchange gives the dominant correction and it is described by the Lagrangian

$$\mathcal{L} = \frac{e\kappa_1}{2M_N} N^\dagger \tau_3 \boldsymbol{\sigma} \cdot \mathbf{B} N, \tag{2.8}$$

where \mathbf{B} is the magnetic field and $\kappa_1 = 2.353$ is the isovector nucleon magnetic moment in nuclear magnetons. These N²LO interactions must be included in the $M1_V$ amplitude. We implicitly include the magnetic moment interactions by using the experimental value $a^{exp} = -23.75$ fm [20]. Also the effective range $r_0 = 2.73$ fm is used. We use the isospin averaged value of the nucleon mass, $M_N = 938.92$ MeV.

B. Lagrangian: \mathcal{L}_2^P

Now, the second Lagrangian \mathcal{L}_2^P is described. For the $E1_V$ transition amplitude, there are also initial or final state nucleon-nucleon interactions in relative angular momentum states 3P_0 , 3P_1 , 3P_2 [3] described by the Lagrangian:

$$\begin{aligned} \mathcal{L}_2^P = & \left(C_2^{(3P_0)} \delta_{xy} \delta_{wz} + C_2^{(3P_1)} [\delta_{xw} \delta_{yz} - \delta_{xz} \delta_{yw}] + C_2^{(3P_2)} \left[2\delta_{xw} \delta_{yz} + 2\delta_{xz} \delta_{yw} - \frac{4}{3} \delta_{xy} \delta_{wz} \right] \right) \\ & \times \frac{1}{4} (N^T \mathcal{O}_{xy}^{(1,P)} N)^\dagger (N^T \mathcal{O}_{wz}^{(1,P)} N) , \end{aligned} \quad (2.9)$$

where the P -wave operator is

$$\mathcal{O}_{ij}^{(1,P)} = \overleftarrow{\mathbf{D}}_i P_j^{(P)} - P_j^{(P)} \overrightarrow{\mathbf{D}}_i \quad (2.10)$$

and $P_i^{(P)}$ are the spin-isospin projectors for the isotriplet, spintriplet channel

$$P_i^{(P)} \equiv \frac{1}{\sqrt{8}} \sigma_2 \sigma_i \tau_2 \tau_3 , \quad \text{Tr} [P_i^{(P)} P_j^{(P)}] = \frac{1}{2} \delta_{ij} . \quad (2.11)$$

The power counting of the P -state couplings is straightforward. Since there are no fine tuned high energy scales in the P -state scattering, the couplings that are dependent on only high energy physics are $\mathcal{O}(1)$ i.e. they do not scale with Q . So, the next set of P -state operators, suppressed by two extra powers of momentum p , enters only at N⁵LO. Only the linear combination

$$C_p \equiv C_2^{(3P_0)} + 2C_2^{(3P_1)} + \frac{20}{3} C_2^{(3P_2)} \quad (2.12)$$

enters our calculation and Nijmegen phase shift analysis [9,21] fixes $C_p = -1.49 \text{ fm}^4$ [3].

C. Lagrangian: \mathcal{L}_2^{EM}

Finally, we discuss the two-body currents contributing to $np \rightarrow d\gamma$ or $\gamma d \rightarrow np$, which are not included in the two previous Lagrangians \mathcal{L}_2^S and \mathcal{L}_2^P . These operators are not related by gauge transformation to the nucleon-nucleon scattering operators in \mathcal{L}_2^S and \mathcal{L}_2^P .

$$\begin{aligned} \mathcal{L}_2^{EM} = & e L_1^{M1_V} (N^T P_i N)^\dagger (N^T \overline{P}_3 N) \mathbf{B}_i - e L_3^{M1_V} (N^T \mathcal{O}_i^{(2)} N)^\dagger (N^T \overline{P}_3 N) \mathbf{B}_i \\ & - e \tilde{L}_3^{M1_V} (N^T P_i N)^\dagger (N^T \overline{\mathcal{O}}_3^{(2)} N) \mathbf{B}_i + \frac{1}{2} e L_1^{E1_V} (N^T \mathcal{O}_{ia}^{(1,P)} N)^\dagger (N^T P_a N) \mathbf{E}_i \\ & - \frac{1}{2} e L_3^{E1_V} (N^T \mathcal{O}_{ia}^{(1,P)} N)^\dagger (N^T \mathcal{O}_a^{(2)} N) \mathbf{E}_i - \frac{1}{2} e \tilde{L}_3^{E1_V} (N^T \mathcal{O}_{ia}^{(3,P)} N)^\dagger (N^T P_a N) \mathbf{E}_i \quad (2.13) \\ & + \frac{1}{2} e L_5^{E1_V} (N^T \mathcal{O}_{ia}^{(1,P)} N)^\dagger (N^T \mathcal{O}_a^{(4)} N) \mathbf{E}_i + \frac{1}{2} e \tilde{L}_5^{E1_V} (N^T \mathcal{O}_{ia}^{(3,P)} N)^\dagger (N^T \mathcal{O}_a^{(2)} N) \mathbf{E}_i \\ & - e L_2^{M1_S} i \epsilon_{ijk} (N^T P_i N)^\dagger (N^T P_j N) \mathbf{B}_k + h.c. , \end{aligned}$$

where \mathbf{E} and \mathbf{B} are the electric and magnetic fields respectively, and

$$\begin{aligned}
\bar{P}_i &= \frac{1}{\sqrt{8}} \sigma_2 \otimes \tau_2 \tau_i \\
\bar{\mathcal{O}}_i^{(2)} &= \frac{1}{4} \left[\overleftarrow{\mathbf{D}}^2 \bar{P}_i - 2 \overleftarrow{\mathbf{D}} \bar{P}_i \overrightarrow{\mathbf{D}} + \bar{P}_i \overrightarrow{\mathbf{D}}^2 \right] \\
\mathcal{O}_{ij}^{(3,P)} &= \frac{1}{4} \left[\overleftarrow{\mathbf{D}}_i \overleftarrow{\mathbf{D}}^2 P_j^{(P)} - 2 \overleftarrow{\mathbf{D}}_i \overleftarrow{\mathbf{D}}_k P_j^{(P)} \overrightarrow{\mathbf{D}}_k + \overleftarrow{\mathbf{D}}_i P_j^{(P)} \overrightarrow{\mathbf{D}}^2 \right. \\
&\quad \left. - \overrightarrow{\mathbf{D}}^2 P_j^{(P)} \overrightarrow{\mathbf{D}}_i + 2 \overrightarrow{\mathbf{D}}_k P_j^{(P)} \overrightarrow{\mathbf{D}}_k \overleftarrow{\mathbf{D}}_i - P_j^{(P)} \overrightarrow{\mathbf{D}}^2 \overrightarrow{\mathbf{D}}_i \right].
\end{aligned} \tag{2.14}$$

The superscript on the two-body current couplings L 's denote the transitions that the particular operators contribute to. For the $M1_V$ transition only a specific p independent combination of $L_1^{M1_V}$ and $L_3^{M1_V}$ contributes and we fix it from the cold neutron capture rate $np \rightarrow d\gamma$. Renormalization group (RG) flow analysis determine $\tilde{L}_3^{M1_V}$ in terms $L_1^{M1_V}$, $C_2^{(1S_0)}$ and $C_2^{(3S_0)}$. For the $E1_V$ transition, only a combination, L_{E1} , of $L_1^{E1_V}$, $L_3^{E1_V}$ and $L_5^{E1_V}$ enters the calculation at N⁴LO and it is fixed from a χ^2 fit to the related deuteron breakup process $\gamma d \rightarrow np$ [3]. The other operators contribute at orders higher than considered here. The RG analysis of these operators is discussed in more detail below. Finally, the observed value of the deuteron magnetic moment μ_M fixes the isoscalar magnetic moment coupling $L_2^{(M1_S)} = -0.149 \text{ fm}^4$ [5,22].

In the last three subsections, we described the Lagrangian and the power counting rules relevant to our calculation. Now, the calculation for the total cross section is presented, along with the estimated theoretical uncertainty. This is followed by the discussion of a matching procedure for determining the unknown couplings $L_1^{M1_V}$ and $L_3^{M1_V}$. The parameter L_{E1} is fixed from the $\gamma d \rightarrow np$ data.

III. CALCULATION AND ANALYSIS

The amplitude Γ for low energy $np \rightarrow d\gamma$ [11,12] is

$$\begin{aligned}
i \Gamma &= e X_{E1_V} U^T \tau_2 \tau_3 \sigma_2 \sigma \cdot \epsilon_{(d)}^* U \mathbf{p} \cdot \epsilon_{(\gamma)}^* + ie X_{M1_V} \epsilon^{abc} \epsilon_{(d)}^{*a} \mathbf{k}^b \epsilon_{(\gamma)}^{*c} U^T \tau_2 \tau_3 \sigma_2 U \\
&\quad + e X_{M1_S} \frac{1}{\sqrt{2}} U^T \tau_2 \sigma_2 \left[\sigma \cdot \mathbf{k} \epsilon_{(d)}^* \cdot \epsilon_{(\gamma)}^* - \epsilon_{(d)}^* \cdot \mathbf{k} \epsilon_{(\gamma)}^* \cdot \sigma \right] U \\
&\quad + e X_{E2_S} \frac{1}{\sqrt{2}} U^T \tau_2 \sigma_2 \left[\sigma \cdot \mathbf{k} \epsilon_{(d)}^* \cdot \epsilon_{(\gamma)}^* + \epsilon_{(d)}^* \cdot \mathbf{k} \epsilon_{(\gamma)}^* \cdot \sigma - \frac{2}{n-1} \sigma \cdot \epsilon_{(d)}^* \mathbf{k} \cdot \epsilon_{(\gamma)}^* \right] U
\end{aligned} \tag{3.1}$$

where only the lowest partial waves are shown: isovector electric dipole capture of nucleons in a P -wave with amplitude X_{E1_V} , isovector magnetic capture of nucleons in 1S_0 state with amplitude X_{M1_V} , isoscalar magnetic capture of nucleons in 3S_1 state with amplitude X_{M1_S} and isoscalar electric quadrupole capture of nucleons with amplitude X_{E2_S} . We use dimensional regularization to regulate divergences and n represents the number of space-time dimensions. The U 's are the nucleon two component spinors. $|\mathbf{p}| \equiv p$ is the nucleon center of mass momentum, k is the outgoing photon momentum, and $\epsilon_{(\gamma)}$ and $\epsilon_{(d)}$ are the photon and deuteron polarization vectors respectively. The following dimensionless amplitudes, \tilde{X} , are defined

$$\begin{aligned}
\frac{|\mathbf{p}|M_N}{\gamma^2 + p^2} X_{E1_V} &= i \frac{2}{M_N} \sqrt{\frac{\pi}{\gamma^3}} \tilde{X}_{E1_V}, & X_{M1_V} &= i \frac{2}{M_N} \sqrt{\frac{\pi}{\gamma^3}} \tilde{X}_{M1_V} \\
X_{M1_S} &= i \frac{2}{M_N} \sqrt{\frac{\pi}{\gamma^3}} \tilde{X}_{M1_S}, & X_{E2_S} &= i \frac{2}{M_N} \sqrt{\frac{\pi}{\gamma^3}} \tilde{X}_{E2_S},
\end{aligned} \tag{3.2}$$

and the total cross section for $np \rightarrow d\gamma$ is then written as:

$$\begin{aligned}
\sigma &= 4\alpha\pi \left(1 - \frac{2p^4 + 4p^2\gamma^2 + 3\gamma^4}{4M_N^2(p^2 + \gamma^2)} \right) \frac{(\gamma^2 + p^2)^3}{\gamma^3 M_N^4 p} \frac{1}{2} \int_{-1}^1 d\cos\theta \left[\frac{3}{2} |\tilde{X}_{E1_V}|^2 \sin^2\theta + |\tilde{X}_{M1_V}|^2 \right. \\
&\quad \left. + |\tilde{X}_{M1_S}|^2 + |\tilde{X}_{E2_S}|^2 \right] \tag{3.3} \\
&\equiv 4\alpha\pi \left(1 - \frac{2p^4 + 4p^2\gamma^2 + 3\gamma^4}{4M_N^2(p^2 + \gamma^2)} \right) \frac{(\gamma^2 + p^2)^3}{\gamma^3 M_N^4 p} \left[\langle \tilde{X}_{E1_V} \rangle^2 + \langle \tilde{X}_{M1_V} \rangle^2 + \langle \tilde{X}_{M1_S} \rangle^2 + \langle \tilde{X}_{E2_S} \rangle^2 \right],
\end{aligned}$$

where the deuteron mass is $M_d \approx 2M_N - \gamma^2/M_N$ [5]. The relativistic corrections enter at N⁴LO and so only the $E1_V$ cross section which is calculated up to this order receives such a contribution.

A. Isovector electric transition $E1_V$

The $E1_V$ amplitude up to N⁴LO is

$$\begin{aligned}
\tilde{X}_{E1_V} &= -\frac{M_N p \gamma^2}{(p^2 + \gamma^2)^2} \left[1 + \frac{\rho_d \gamma}{2} + \frac{3}{8} \rho_d^2 \gamma^2 + \frac{5}{16} \rho_d^3 \gamma^3 + \frac{35}{128} \rho_d^4 \gamma^4 - \frac{5}{2} \eta_d^2 + \frac{(p^2 + \gamma^2)^2}{2M_N} L_{E1} \right. \\
&\quad + \frac{M_N \gamma}{12\pi} \left(\frac{\gamma^2}{3} + p^2 \right) C_p \left(1 + \frac{\rho_d \gamma}{2} \right) + \frac{|p|}{M_N} \cos\theta \left(1 + \frac{\rho_d \gamma}{2} + \frac{3}{8} \rho_d^2 \gamma^2 \right) \\
&\quad \left. + \frac{p^2}{M_N^2} \cos^2\theta - \frac{8p^4 + 17p^2\gamma^2 + 5\gamma^4}{16M_N^2(p^2 + \gamma^2)} \right], \tag{3.4}
\end{aligned}$$

where the relativistic corrections contribute at N⁴LO as they are suppressed by additional powers of $(m_\pi/M_N)^2$, and

$$\begin{aligned}
L_{E1} &\equiv \frac{L_{1,-1}^{E1} - \gamma^2 L_{3,-3}^{E1} + \gamma^4 L_{5,-5}^{E1} + \gamma^4 M_N (C_{8,-5}^\beta + 2C_{8,-5}^{(3S_1)}) - M_N \eta \tilde{C}_{4,-1}}{C_{0,-1}^{(3S_1)}} \tag{3.5} \\
\eta \tilde{C}_{4,-1} &\equiv \tilde{C}_{4,-1}^{(3S_1)} + \frac{2\pi}{M_N} \frac{\rho_d w_2 \gamma^2}{(\mu - \gamma)^3}.
\end{aligned}$$

The $\eta \tilde{C}_{4,-1}$ coupling renormalizes contributions proportional to η_d^2 in Eq. (3.4). The μ independent parameter $L_{E1} \sim \mathcal{O}(1)$ can be simplified further. We assume that all the couplings have a sensible large scattering length ($\gamma \rightarrow 0$) limit. Then it follows that at the high scale $\mu = \Lambda$, only the combination $(L_{1,-1}^{E1} - M_N \eta \tilde{C}_{4,-1})/C_{0,-1}^{(3S_1)}$ contributes a $\mathcal{O}(1)$ term. The other combinations, e.g. $\gamma^2 L_{3,-3}^{E1}/C_{0,-1}^{(3S_1)}$, contribute terms of $\mathcal{O}(Q^2)$ and higher. Thus RG analysis gives

$$L_{E1} \equiv \frac{L_{1,-1}^{E1} - M_N \eta \tilde{C}_{4,-1}}{C_{0,-1}^{(3S_1)}} (1 + \mathcal{O}(Q^2)), \quad (3.6)$$

and we keep only the LO contribution to L_{E1} for our calculation. It is possible to make an order of magnitude estimate for L_{E1} . The contribution from S - D mixing, proportional to η_d^2 , is numerically negligible at N⁴LO even though it is formally a N⁴LO term. Thus, ignoring contribution from $\eta \tilde{C}_{4,-1}$, we estimate at the renormalization $\mu = \Lambda \sim m_\pi/2$

$$\begin{aligned} |C_{0,-1}^{(3S_1)}| &\sim \frac{4\pi}{M_N \Lambda}, & |L_{1,-1}^{E1}| &\sim \frac{1}{M_N \Lambda^4} \\ \Rightarrow |L_{E1}| &\sim 2 \text{ fm}^3, \end{aligned} \quad (3.7)$$

where factors of $1/M_N$ from the nucleon loops were included.

In Eq. (3.4), we have only kept the terms that contribute to the total cross section after summing over deuteron, photon and nucleon polarizations. We have included the formally N²LO contribution proportional to $\cos \theta$. This term, odd in $\cos \theta$, contributes to the cross section only at N⁴LO after the integration over the angle θ , Eq. (3.3). In obtaining Eq. (3.4), we have also used the fact that only the μ independent combination

$$\frac{\tilde{L}_{3,-3}^{(E1_V)} - \gamma^2 \tilde{L}_{5,-5}^{(E1_V)} - 2M_N \tilde{C}_{6,-3}^{(3S_1)} + 2M_N \gamma^2 C_{8,-5}^\beta}{C_{0,-1}^{(3S_1)}} \quad (3.8)$$

enters our result. From RG analysis, by flowing the couplings to the high scale $\mu = \Lambda$, we see that the numerator is $\mathcal{O}(1/Q)$ instead of the naive counting of $1/Q^3$. Thus this particular combination of operators contributes starting at N⁶LO and we ignore it in this N⁴LO calculation.

The dominant contribution beyond leading order, Eq. (3.4), is a simple expansion of the factor $\sqrt{Z_d} \equiv 1/\sqrt{1 - \rho_d \gamma}$ from the deuteron wave function renormalization

$$\mathcal{Z} = -\frac{8\pi\gamma}{M_N^2} \left[1 + \rho_d \gamma + \rho_d^2 \gamma^2 + \rho_d^3 \gamma^3 + \rho_d^4 \gamma^4 + \eta_d^2 \frac{7\gamma - 5\mu}{\mu - \gamma} + \frac{\gamma^2}{8M_N^2} \frac{7\mu - 5\gamma}{\mu - \gamma} + \dots \right]. \quad (3.9)$$

In Eq. (3.9), the $\rho_d \gamma$ terms inside the square brackets are from the expansion of Z_d , and the second and third terms arise from the S - D mixing and relativistic corrections to the deuteron two-point function respectively.

Amplitudes for inelastic processes, e.g. $E1_V$ and $M1_V$ transitions, with a deuteron in the final state involve a factor of $\sqrt{Z_d}$. On the other hand amplitudes for elastic processes involving a deuteron, e.g. the deuteron quadrupole form factor F_Q , include a factor of Z_d . In Ref. [6], an expansion in $Z_d - 1$ was proposed which resums the expansion in $\rho_d \gamma$ seen in Eq. (3.9) and thereby reproduces the exact factor of Z_d at NLO for the amplitude for elastic processes. On the other hand, amplitudes involving inelastic processes on the deuteron have this sum incomplete. The factor of $\sqrt{Z_d}$ is reproduced only in perturbation. This incomplete sum can be avoided if we do an expansion in $\sqrt{Z_d} - 1$ to reproduce the exact factor of $\sqrt{Z_d}$ for inelastic processes. The overall factor of Z_d in elastic processes is then reproduced at N²LO instead of NLO. Thus, one might think that the $\sqrt{Z_d} - 1$ expansion is more appropriate to calculate the cross section for the inelastic process $np \rightarrow d\gamma$. However,

for the total cross section, which is summed over the nucleon spins and the deuteron and photon polarizations, it is the square of the amplitudes that enter the expression. In such cases it is more convenient to do the expansion in $Z_d - 1$ and reproduce the exact factor of Z_d at NLO. The three different expansions $\rho_d\gamma$, $Z_d - 1$, $\sqrt{Z_d} - 1$ are formally equivalent but correspond to different ways of relating the C_{2n} couplings to the ERE. In the $Z_d - 1$ expansion, the position of the deuteron pole at momentum $p = i\gamma_t \approx i\gamma$ and the residue Z_d (without S - D mixing) at the pole are used to fix the C_{2n} couplings. For rest of the paper we will use the this expansion. The results for \tilde{X} can then be written as:

$$\begin{aligned}
\tilde{X}_{E1\nu} &= -\frac{M_N p \gamma^2}{(p^2 + \gamma^2)^2} \left[1 + \frac{1}{2}(Z_d - 1) - \frac{1}{8}(Z_d - 1)^2 + \frac{1}{16}(Z_d - 1)^3 - \frac{5}{128}(Z_d - 1)^4 \right. \\
&\quad \left. + \frac{M_N \gamma}{12\pi} \left(\frac{\gamma^2}{3} + p^2 \right) C_p \left(1 + \frac{1}{2}(Z_d - 1) \right) - \frac{5}{2}\eta_d^2 + \frac{(p^2 + \gamma^2)^2}{2M_N} L_{E1} \right. \\
&\quad \left. - \frac{8p^4 + 17p^2\gamma^2 + 5\gamma^4}{16M_N^2(p^2 + \gamma^2)} + \frac{|p|}{M_N} \cos\theta \left(1 + \frac{1}{2}(Z_d - 1) - \frac{1}{8}(Z_d - 1)^2 \right) + \frac{p^2}{M_N^2} \cos^2\theta \right] \\
\langle \tilde{X}_{E1\nu} \rangle^2 &= \frac{M_N^2 p^2 \gamma^4}{(p^2 + \gamma^2)^4} Z_d \left[1 + \frac{M_N \gamma}{6\pi} \left(\frac{\gamma^2}{3} + p^2 \right) C_p - \frac{5\eta_d^2}{Z_d} + \frac{(p^2 + \gamma^2)^2}{Z_d M_N} L_{E1} \right. \\
&\quad \left. - \frac{8p^4 + 17p^2\gamma^2 + 5\gamma^4}{8Z_d M_N^2(p^2 + \gamma^2)} + \frac{3}{5} \frac{p^2}{Z_d M_N^2} \right], \tag{3.10}
\end{aligned}$$

where the last part in $\langle \tilde{X}_{E1\nu} \rangle^2$ is from the $\cos^2\theta$ terms.

The expression for $\langle \tilde{X}_{E1\nu} \rangle^2$ in Eq. (3.10) is a perturbative result. There are corrections to this expression from terms that are higher order than the ones considered here in the perturbative expansion. The higher order corrections can be separated into (a) factors of Z_d from the wavefunction renormalization of the deuteron, Eq. (3.9) and (b) contributions from higher order nucleon-nucleon scattering operators and two-body currents. At $E \sim 1$ MeV, we expect higher order corrections to contribute $(Z_d - 1)(p^2 + \gamma^2)/M_N^2 \sim 0.004$, $5(Z_d - 1)\eta_d^2 \sim 0.002$ due to wave function renormalization. The $Z_d - 1$ corrections to the term involving L_{E1} are renormalized away when we fit L_{E1} . The higher order P -wave operators should contribute $M_N \gamma p^4 / (6\pi\Lambda^6) \sim 0.01$ with $\Lambda \sim m_\pi/2$. Thus we estimate the theoretical error to be $\sim 1\%$ at energies of $E \sim 1$ MeV. The error is smaller at lower energies.

B. Isovector magnetic transition $M1\nu$

A straight forward calculation of $M1\nu$ amplitude gives:

$$\begin{aligned}
\tilde{X}_{M1\nu}^{(0)} &= -\kappa_1 \gamma^2 \left(\frac{1}{p^2 + \gamma^2} - \frac{1}{(\gamma - ip) \left(\frac{1}{a^{exp}} + ip \right)} \right) \\
\tilde{X}_{M1\nu}^{(1)} &= \frac{1}{2}(Z_d - 1)\tilde{X}_{M1\nu}^{(0)} + \kappa_1 \frac{r_0}{2} \frac{p^2 \gamma^2}{\left(\frac{1}{a^{exp}} + ip \right)^2 (\gamma - ip)} + \frac{\gamma^2 M_N}{4\pi \left(\frac{1}{a^{exp}} + ip \right)} L_{np} \tag{3.11} \\
\tilde{X}_{M1\nu}^{(2)} &= \left(\frac{1}{2}(Z_d - 1) + \frac{r_0}{2} \frac{p^2}{\frac{1}{a^{exp}} + ip} \right) [\tilde{X}_{M1\nu}^{(1)} - \frac{1}{2}(Z_d - 1)\tilde{X}_{M1\nu}^{(0)}] \\
&\quad - \frac{1}{8}(Z_d - 1)^2 \tilde{X}_{M1\nu}^{(0)} + \frac{M_N}{4\pi} \frac{\gamma^2}{\frac{1}{a^{exp}} + ip} \tilde{L}_{np},
\end{aligned}$$

where the μ independent parameters are

$$\begin{aligned}
L_{np} &\equiv (\mu - \gamma)(\mu - 1/a^{exp}) \left[L_{1,-2}^{M1_V} - \frac{\kappa_1 \pi}{M_N \gamma} \left(\frac{r_0 \gamma}{(\mu - \frac{1}{a^{exp}})^2} + \frac{Z_d - 1}{(\mu - \gamma)^2} \right) \right] \\
\tilde{L}_{np} &\equiv (\mu - \gamma)(\mu - 1/a^{exp}) \left[L_{1,-1}^{M1_V} - \gamma^2 L_{3,-3}^{M1_V} + \frac{\kappa_1 \pi}{M_N \gamma} \frac{(Z_d - 1)^2}{(\mu - \gamma)^2} \right] \\
&= (\mu - \gamma)(\mu - 1/a^{exp}) \left[L_{1,-1}^{M1_V} + \frac{\kappa_1 \pi}{M_N \gamma} \frac{(Z_d - 1)^2}{(\mu - \gamma)^2} \right] (1 + \mathcal{O}(Q^2)) .
\end{aligned} \tag{3.12}$$

An analysis similar to the one used for L_{E1} , allows us to simplify the parameters L_{np} above in Eq. (3.12). A naive estimate gives

$$-9.5 \text{ fm}^2 \lesssim L_{np} \lesssim -8.3 \text{ fm}^2 , \quad 2.8 \text{ fm}^2 \lesssim \tilde{L}_{np} \lesssim 3.6 \text{ fm}^2 . \tag{3.13}$$

We use the experimentally measured scattering length a^{exp} which includes the effect of single magnetic photon exchange in neutron-proton scattering. In Eq. (3.11), from RG analysis, we used:

$$\tilde{L}_{3,-3}^{M1_V} = \frac{\xi}{(\mu - \gamma)(\mu - \frac{1}{a^{exp}})} - \frac{r_0}{2} \frac{1}{\mu - \frac{1}{a^{exp}}} \left[L_{1,-2}^{M1_V} + \frac{\kappa_1 \pi}{M_N \gamma} \left(\frac{r_0 \gamma}{(\mu - \frac{1}{a^{exp}})^2} - \frac{Z_d - 1}{(\mu - \gamma)^2} \right) \right] . \tag{3.14}$$

The first part $\mathcal{O}(1/Q^2)$ gives higher order corrections to $\tilde{L}_3^{M1_V} \sim 1/Q^3$ and we can set $\xi = 0$ at N⁴LO, and have $\tilde{L}_3^{M1_V}$ completely determined. Up to N²LO

$$|\tilde{X}_{M1_V}|^2 = |\tilde{X}_{M1_V}^{(0)}|^2 + 2Re[\tilde{X}_{M1_V}^{(0)}(\tilde{X}_{M1_V}^{(1)})^*] + |\tilde{X}_{M1_V}^{(1)}|^2 + 2Re[\tilde{X}_{M1_V}^{(0)}(\tilde{X}_{M1_V}^{(2)})^*] . \tag{3.15}$$

The singlet channel scattering length $a^{exp} = -23.75 \text{ fm}$ is unnaturally large and it is easier to do the error analysis for the cross section in the limit $a^{exp} \rightarrow \infty$, with finite corrections from $1/(a^{exp}\gamma)$ and $1/(a^{exp}p)$ terms. There are corrections from initial state interactions in the 1S_0 channel that come in as $r_0^3 p^6 / \gamma^3 \sim 0.03$ at center of mass energy $E = 1 \text{ MeV}$. The momentum independent corrections from factors of $Z_d - 1$ from deuteron wavefunction renormalization, $r_0 \gamma$ from 1S_0 channel initial state interaction etc. get renormalized away when we fit the parameters L_{np} 's at very low momentum. There is also a contribution from 1S_0 operators that come in as $r_1 p^4 / \gamma \sim -0.002$, where the shape parameter $r_1 \sim -1 \text{ fm}^3$ is the 1S_0 equivalent of w_2 in Eq. (2.7). We estimate the errors in $M1_V$ to be $\sim 3\%$ at $E = 1 \text{ MeV}$.

C. Isoscalar magnetic and electric transitions $M1_S$, $E2_S$

The $M1_S$ and $E2_S$ amplitude have been calculated [11,12] for cold neutron capture. The leading contribution from these transitions at non-zero momentum transfer is:

$$\begin{aligned}
|\tilde{X}_{M1_S}|^2 &= \frac{M_N^2 \gamma^4}{2\pi^2(p^2 + \gamma^2)} (L_2^{M1_S})^2 (\gamma - \mu)^4 \\
|\tilde{X}_{E2_S}|^2 &= \frac{\gamma^4 \eta_d^2}{100} \frac{(p^4 + 7p^2 \gamma^2 + \gamma^4)}{(p^2 + \gamma^2)^4} .
\end{aligned} \tag{3.16}$$

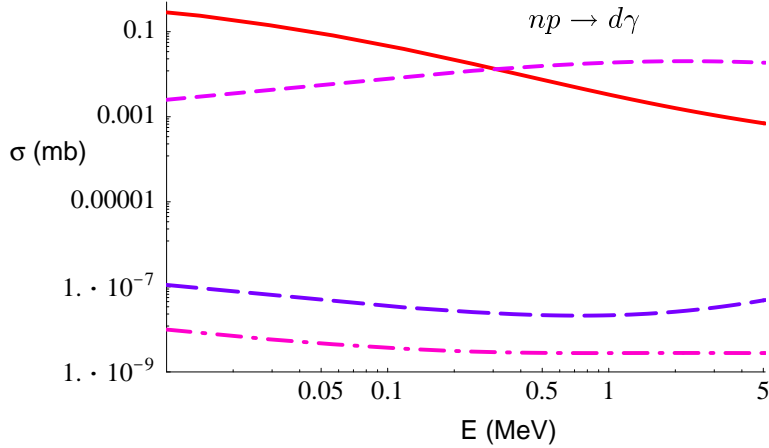


FIG. 1. $np \rightarrow d\gamma$ transition cross section σ (mb) for center of mass energy E (MeV), on a log-log plot. Solid curve: LO $M1_V$ transitions, dash: LO $E1_V$ transitions, long-dash: LO $M1_S$ transitions and dot-dash: LO $E2_S$ transitions.

The coupling $L_2^{M1_S}$ can be fitted to the deuteron magnetic moment at the renormalization scale $\mu = m_\pi$ and gives $L_2^{M1_S}(m_\pi) = -0.149 \text{ fm}^4$ [5,22].

In the last three subsections, the $np \rightarrow d\gamma$ amplitude in terms of the lowest partial waves, $M1_V$, $E1_V$, $M1_S$ and $E2_S$ has been calculated in terms of three unknown parameters L_{np} , \tilde{L}_{np} and L_{E1} Eqs. (3.10), (3.11). Thus we now move on to describe how the three unknown parameters L_{np} , \tilde{L}_{np} and L_{E1} can be determined from $np \rightarrow d\gamma$ for cold neutrons and from photodisintegration of the deuteron $\gamma d \rightarrow np$.

D. Determining the parameters L_{np} , \tilde{L}_{np} and L_{E1}

The leading contributions from each partial wave are shown in Fig. 1. One can see that the $M1_S$ and $E2_S$ transitions can be ignored for a 1% level calculation in the energy range of interest. At center of mass momentum $p_0 = 0.003443 \text{ MeV}$ the cross section for $np \rightarrow d\gamma$ is measured to be $\sigma^{exp} = 334.2 \pm 0.5 \text{ mb}$ [13] and $M1_V$ transitions give the dominant contribution, Fig. 1. Thus at NLO, we fix L_{np} from this cold neutron capture rate:

$$\begin{aligned} \sigma^{(LO)} &\equiv \frac{4\pi\alpha(\gamma^2 + p^2)^3}{\gamma^3 M_N^4 p} |\tilde{X}_{M1_V}^{(0)}|^2 \Big|_{p=p_0} \\ \sigma^{(NLO)} &\equiv \sigma^{exp} - \sigma^{(LO)} = \frac{4\pi\alpha(\gamma^2 + p^2)^3}{\gamma^3 M_N^4 p} 2\text{Re}e(\tilde{X}_{M1_V}^{(0)}(\tilde{X}_{M1_V}^{(1)})^*) \Big|_{p=p_0} \\ &\Rightarrow L_{np} = -9.039 \pm 0.027 \text{ fm}^2 . \end{aligned} \quad (3.17)$$

The N²LO terms also contribute to the cross section at momentum p_0 . So, we impose the constraint [14]

$$\sigma^{(NNLO)} \equiv \frac{4\pi\alpha(\gamma^2 + p^2)^3}{\gamma^3 M_N^4 p} \left[|\tilde{X}_{M1_V}^{(1)}|^2 + 2\text{Re}e(\tilde{X}_{M1_V}^{(0)}(\tilde{X}_{M1_V}^{(2)})^*) \right] \Big|_{p=p_0} = 0 , \quad (3.18)$$

to reproduce the experimental cross section σ^{exp} . This determines the parameter $\tilde{L}_{np} = 4.957 \pm 0.011 \text{ fm}^2$. The parameter L_{E1} , which contributes only to $E1_V$ transitions, can not

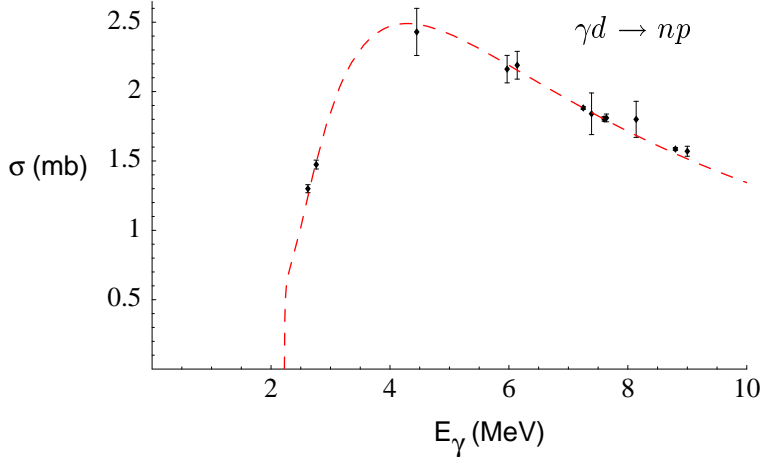


FIG. 2. Cross section in mb for $\gamma d \rightarrow np$ as a function of photon energy E_γ in MeV. The data is taken from Ref. [15], pages 78 and 79.

be determined reliably from this single data point since the $E1_V$ cross section is negligible at this low momentum p_0 . The error due to the experimental uncertainty in σ^{exp} is significant for energy $E \lesssim 0.25$ MeV. Above this energy the $E1_V$ cross section gives the dominant contribution and the error in $M1_V$ cross section can be ignored. The contribution of the four-nucleon-one-photon counterterm is found to be significant at low momentum $p_0 = 0.003443$ MeV. Neglecting the counterterm by setting $L_1^{M1_V} = 0$ at NLO underpredicts the experimental result σ^{exp} by 5%. This number is different from the one quoted in Ref. [5,11], where the $\rho_d\gamma$ expansion was used.

The parameter L_{E1} can be determined from photodisintegration of the deuteron. This cross section is related to the neutron capture cross section [3,15] by

$$\sigma(\gamma d \rightarrow np) = \frac{2M_N}{3E_\gamma^2} \left[E_\gamma - B + \frac{B^2 - 6BE_\gamma + 4E_\gamma^2}{4M_N} \right] \sigma(np \rightarrow d\gamma), \quad (3.19)$$

where E_γ is the incident photon energy in the deuteron rest frame. Only the $E1_V$ transitions, on the right hand side of Eq. (3.19), receive relativistic corrections. In principle it is possible to determine all the three parameters L_{np} , \tilde{L}_{np} and L_{E1} from the deuteron breakup data. However, in the nucleon energy range $0.3 \text{ MeV} \lesssim E \approx E_\gamma - B \lesssim 0.5 \text{ MeV}$, there are only two data points, Fig. 2, and such a determination leads to significant uncertainty in the dominant $M1_V$ cross section. We find that a χ^2 fit to data [15] in the photon energy range $2.6 \text{ MeV} < E_\gamma < 7.3 \text{ MeV}$ does not give a reliable constraint on the parameters L_{np} , \tilde{L}_{np} and L_{E1} . Constraining L_{np} and \tilde{L}_{np} from σ^{exp} as described above determines them more accurately. The other parameter L_{E1} is determined from a χ^2 fit to data [15] in the photon energy range $2.6 \text{ MeV} < E_\gamma < 7.3 \text{ MeV}$, where experimental errors in the $M1_V$ cross section are negligible. This gives:

$$L_{E1} = -(5.3 \pm 3.6) \text{ fm}^3. \quad (3.20)$$

The error due to experimental uncertainty is $\lesssim 1\%$ over the range of $E \lesssim 5$ MeV. This means that for nucleon energies $E \lesssim 0.4$ MeV, the experimental uncertainty is significant compared to theoretical error, see Fig. 3. A few more high precision measurements in the incident

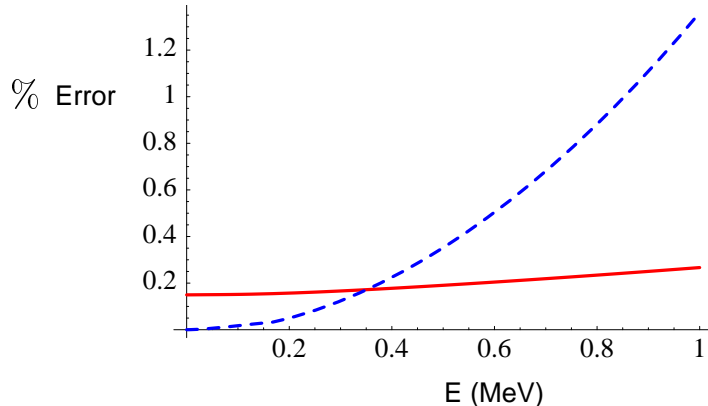


FIG. 3. Estimated theoretical error and experimental uncertainty in the cross section $np \rightarrow d\gamma$. The errors are shown in percentages versus nucleon center of mass energy E (MeV). Solid curve: experimental uncertainty, dotted curve: estimated theoretical error.

photon energy range $2.5 \text{ MeV} \lesssim E_\gamma \lesssim 5 \text{ MeV}$ would provide important constraints on L_{E1} and determine the $np \rightarrow d\gamma$ cross section more accurately at energies relevant for big-bang nucleosynthesis.

The contribution from N⁴LO is found to be $\lesssim 3\%$ for incident photon energies $E_\gamma \lesssim 8 \text{ MeV}$ and is a small correction to the N³LO result [3]. This is better than the naive theoretical estimate for energies $E_\gamma > 4 \text{ MeV}$. This low energy theory, which is formally valid for energies $E_\gamma \lesssim 8 \text{ MeV}$, seems to reproduce data well above its range of validity, see Fig. 2. We also note that the fitted values of the parameters L_{np} , \tilde{L}_{np} and L_{E1} are consistent with the naive theoretical estimates, Eqs. (3.7), (3.13).

IV. RESULTS

Table I shows the EFT $np \rightarrow d\gamma$ cross section for various nucleon center of mass energies, E . The corresponding values for the cross section from the on-line data center [16] are also shown in the last column. As explained earlier, an error of $r_1 p^4/\gamma + r_0^3 p^6/\gamma^3(1 + |1/(a^{exp}p)| + |1/(a^{exp}\gamma)|)$ with respect to LO was assigned to the $M1_V$ cross section and an error of $M\gamma p^4/(6\pi\Lambda^6) - 5(Z_d - 1)\eta_d^2 + (Z_d - 1)(p^2 + \gamma^2)/M_N^2$ was assigned to the $E1_V$ cross section. The errors were added linearly to the total cross section and are found to be $\lesssim 1\%$ for $E \lesssim 1 \text{ MeV}$. The EFT result is presented to only four significant digits, unless the theoretical error enters earlier, in which case we keep up to the first digit where the error contributes. Compared to the results in Ref. [3], these higher order EFT results are perturbatively closer to the ENDF values. However, at some energies, e.g. $1 \times 10^{-3} \text{ MeV}$, where the difference between the N³LO EFT result and ENDF value is much larger than the expected perturbative corrections [3], not surprisingly the discrepancy does not disappear by going to N⁴LO.

$\sigma(np \rightarrow d\gamma)$				
E (MeV)	$M1_V$ (mb)	$E1_V$ (mb)	$M1_V + E1_V$ (mb)	ENDF (mb) [16]
1.26254×10^{-8}	334.2 *	5.122×10^{-6}	334.2 *	332.0
$5. \times 10^{-4}$	1.667(0)	0.001019(0)	1.668(0)	1.660
$1. \times 10^{-3}$	1.170(0)	0.001441(1)	1.172(0)	1.193
$5. \times 10^{-3}$	0.4950(0)	0.003216(1)	0.4982(0)	0.496
$1. \times 10^{-2}$	0.3279(0)	0.004538(1)	0.3324(0)	0.324
$5. \times 10^{-2}$	0.09810(0)	0.009966(3)	0.1081(0)	0.108
0.100	0.04973(0)	0.01379(0)	0.06352(0)	0.0633
0.500	0.00787(2)	0.02626(6)	0.0341(1)	0.0345
1.00	0.0036(1)	0.0313(3)	0.0349(4)	0.0342

TABLE I. Cross section for $np \rightarrow d\gamma$ in mb for different center of mass energy E (MeV). For comparison, the values from the on line database at NNDC are also shown. The first entry (*) is used for fitting a combination of parameters L_{np} , Eq. (3.12). Another parameter L_{E1} , Eq. (3.5), was fitted to the deuteron photodisintegration $\gamma d \rightarrow np$ cross section.

V. SUMMARY AND CONCLUSIONS

In finale, the big-bang nucleosynthesis prediction for primordial deuterium abundance uses the cross section for $np \rightarrow d\gamma$ as an input. A precise estimate of this cross section is thus critical for predicting the primordial abundance of other light elements. The total cross section for radiative capture of neutrons on the proton $np \rightarrow d\gamma$ was calculated in EFT for center of mass energies $E \lesssim 1$ MeV. At the energies relevant for BBN, $0.02 \text{ MeV} \lesssim E \lesssim 0.2 \text{ MeV}$, the isovector magnetic transition $M1_V$ and the isovector electric transition $E1_V$ give the dominant contributions.

We calculated the $M1_V$ cross section to N²LO and the $E1_V$ cross section to N⁴LO. For the $M1_V$ transition there is a four-nucleon-one-photon counterterm at NLO that is not related to nucleon-nucleon scattering operators by gauge transformations. This term contributes $\sim 2\%$ to the total cross section at $E = 0.5$ MeV. Up to N³LO, the $E1_V$ amplitude calculated in EFT is equivalent to the effective range theory result. However, the effective range theory result differs from the N⁴LO EFT result due to the absence of a four-nucleon-one-photon counterterm. This unknown counterterm is determined from the deuteron breakup $\gamma d \rightarrow np$ data with significant experimental uncertainty. A few more precise measurements in the incident photon energy range $2.5 \text{ MeV} \lesssim E_\gamma \lesssim 5 \text{ MeV}$ would provide important constraints on the $M1_V$ and $E1_V$ transitions in the energies relevant for BBN. For energies $E \lesssim 1$ MeV, the theoretical uncertainty in the total cross section is estimated to be $\lesssim 1\%$.

ACKNOWLEDGMENT

The author would like to thank Jiunn-Wei Chen, Daniel Phillips and Martin Savage for many helpful discussions. We would also like to thank Paulo Bedaque for useful comments on the manuscript, and the other members of the EFT group at the University of Washington for valuable suggestions. This work is supported in part by the U.S. Dept. of Energy under Grant No. DE-FG0397ER4014.

REFERENCES

- [1] S. Burles, K. M. Nollet, J. N. Truran and M.S. Turner, *Phys. Rev. Lett.* **82**, 4176 (1999).
- [2] M.S. Smith, L.H. Kawano and R.A. Malaney, *Astrophys. J. Suppl.Ser.* **85**, 219 (1993).
- [3] J.W. Chen and M.J. Savage, nucl-th/9907042.
- [4] D.B. Kaplan, M.J. Savage and M.B. Wise, *Phys. Lett. B* **424**, 390 (1998), *Nucl. Phys. B* **534**, 329 (1998).
- [5] J.W. Chen, G. Rupak and M.J. Savage, *Nucl. Phys. A* **653**, 386 (1999).
- [6] D.R. Phillips, G. Rupak and M.J. Savage, nucl-th/9908054.
- [7] U. van Kolck, *Nucl. Phys. A* **645**, 273 (1999).
- [8] D.R. Phillips and T.D. Cohen, nucl-th/9906091.
- [9] V.G.J. Stoks, R.A.M. Klomp, C.P.F. Terheggen and J.J. de Swart, *Phys. Rev. C* **49**, 2950 (1994).
- [10] R.B. Wiringa, V.G.J. Stoks and R. Schiavilla, *Phys. Rev. C* **49**, 38 (1995).
- [11] M.J. Savage, K.A. Scaldeferri and M.B. Wise, *Nucl. Phys. A* **652**, 273 (1999).
- [12] J.W. Chen, G. Rupak and M.J. Savage, nucl-th/9905002.
- [13] A.E. Cox, S.A.R. Wynchank and C.H. Collie, *Nucl. Phys.* **74**, 497 (1965).
- [14] G. Rupak and N. Shores, *Phys. Rev. C* **60**, 054004 (1999), nucl-th/9906077.
- [15] H. Arenhovel and M. Sanzone. *Photodisintegration of the Deuteron: A Review of Theory and Experiment*. Number ISBN 3-211-82276-3. Springer-Verlag, 1991.
- [16] ENDF/B online database at the NNDC Online Data Service, <http://www.nndc.bnl.gov>.
- [17] J. Schwinger, Harvard lecture notes. Quoted by J. Blatt, *Phys. Rev.* **74**, 92 (1948). H.A. Bethe, *Phys. Rev.* **76**, 38 (1949).
- [18] J.J. de Swart, C.P.F. Terheggen and V.G.J. Stoks, nucl-th/9509032.
- [19] T.S. Park, K. Kubodera and M. Rho, *Phys. Rev. C* **58**, 637 (1998).
- [20] L. Koester and W. Nistler, *Z. Phys. A* **272**, 189 (1975).
- [21] V.G.J. Stoks, R.A.M. Klomp, M.C.M. Rentmeester and J.J. de Swart, *Phys. Rev. C* **48**, 792 (1993).
- [22] D.B. Kaplan, M.J. Savage and M.B. Wise, *Phys. Rev. C* **59**, 617 (1999).